Structure–Property Relationships in Dendritic Encapsulation

CHRISTOPHER B. GORMAN* AND
JENNIFER C. SMITH

*Department of Chemistry, North Carolina State University,
Box 8204, Raleigh, North Carolina 27695-8204*

Received March 17, 2000

ABSTRACT

Several molecular structure–property relationships are presented and compared to illustrate our current understanding of macromolecular encapsulation using dendrimers. Specifically, the effect that dendrimer architectures have on encapsulating photoactive and redox-active units fixed at the molecular core is considered.

I. Introduction

Dendrimers are novel macromolecules in which regularly branching repeat units emanate out from a central molecular core. Such a configuration results in an exponential increase in molecular weight for a geometric increase in volume. This relationship has led to the hypothesis that, at some critical molecular weight, the molecular core is effectively encapsulated by a sterically crowded, close-packed dendritic architecture.[1-3] By sterically shielding the molecular core from the surrounding environment, several potential useful behaviors might be realized. These include attenuation of luminescence quenching of a photoactive core moiety with applicability in energy collection and transduction schemes,[4-12] and attenuation of electron transfer to and from a redox-active core moiety with applicability in single-molecule binary information storage schemes.[13,14]

Although this Account will focus on encapsulation of the core of the dendrimer, the word "encapsulation" refers generically to several different schemes in dendrimer chemistry. For example, Meijer et al. have reported a so-called "dendritic box" in which small molecules were trapped inside individual dendrimer molecules and subsequently released only when sterically bulky, hydrogen-bonded peripheral groups were cleaved.[15-17] This type of noncovalent encapsulation of small molecules within a

dendrimer architecture has potential applicability in catalysis[18-24] and drug delivery[25-28] schemes. In another example, Zimmerman et al. reported a dendrimer with well-defined hydrogen bond donor–acceptor host units at the molecular core and studied binding properties of guest molecules.[29] These examples are hardly encompassing and are given merely to represent the range of encapsulation schemes reported.

Since dendrimers are almost always difficult or impossible to characterize structurally in an unambiguous way (e.g., by X-ray crystallography), more or less all discussion of encapsulation is derived from the effect the architecture has on some type of probe. In the particular case of interest here, where the core of the dendrimer is encapsulated, a core that is electroactive or photoactive is almost always employed. The effect of the repeat unit structure and degree of hyperbranching in the dendrimer on the redox or photophysical properties of the core unit can then be studied. These effects comprise macromolecular structure–property relationships for dendritic encapsulation.

Photoactive and redox-active core dendrimers are, in many instances, reminiscent of metalloproteins.[30-40] In both cases, encapsulation of a metal center or metal cluster results in dramatic changes in its physical properties. In redox proteins, for example, dramatic shifts in thermodynamic redox potential can be observed as a function of relative solvent accessibility and relative charge destabilization at the metal center.[41] The extent to which similar effects are observed in metallodendrimers, and thus the degree of applicability of these molecules in mimicking the behavior of a metalloprotein, is probed here.

In this Account, the efforts to study the effects of bonding a dendritic architecture around electroactive and photoactive cores are critically discussed. In the case of core redox potential, it will be illustrated that issues that are considered in proteins (relative solvent accessibility and relative charge destabilization of redox centers) are generally applicable to rationalizing redox potential changes in dendrimers. Not all redox-active moieties display a change in redox potential as the amount of dendritic coating around them is increased, and a model explaining these apparently conflicting results is advanced. When considering kinetic phenomena such as attenuation of electron-transfer rate with increasing molecular size, the conformation and, more importantly, conformational flexibility of the dendrimer must be taken into account. These effects and their results are illustrated herein.

II. Encapsulation of the Dendritic Core

A. Influencing Redox Potentials in Electroactive Core Dendrimers. Nature has the unique ability to control redox potentials in metalloproteins by tuning the microenvironment surrounding a metal center or metal

Christopher Gorman was born in Summit, NJ, in 1965. He received his B.A. in chemistry and computer science from Drew University in 1987 and his Ph.D. in chemistry from the California Institute of Technology in 1991, working under Professor Robert Grubbs. He then did postdoctoral work with Dr. Seth Marder at the NASA Jet Propulsion Laboratory and with Professor George Whitesides at Harvard University. He is now Associate Professor of Chemistry at North Carolina State University. His research interests are in the design and synthesis of new materials with interesting and useful electronic properties at nanometer length scales and the use of scanned probe microscopies in nanoscience.

Jennifer Smith was born in Goldsboro, NC, in 1972. She obtained her B.A. in chemistry from University of North Carolina at Chapel Hill in 1994 and her Ph.D. from North Carolina State University in 1999. Her research interests lie in organic materials chemistry and electron transfer in organic chemistry and biochemistry.

* To whom correspondence should be addressed. Telephone: (919) 515-4252. Fax: (919) 515-8920. E-mail: Chris_Gorman@ncsu.edu.
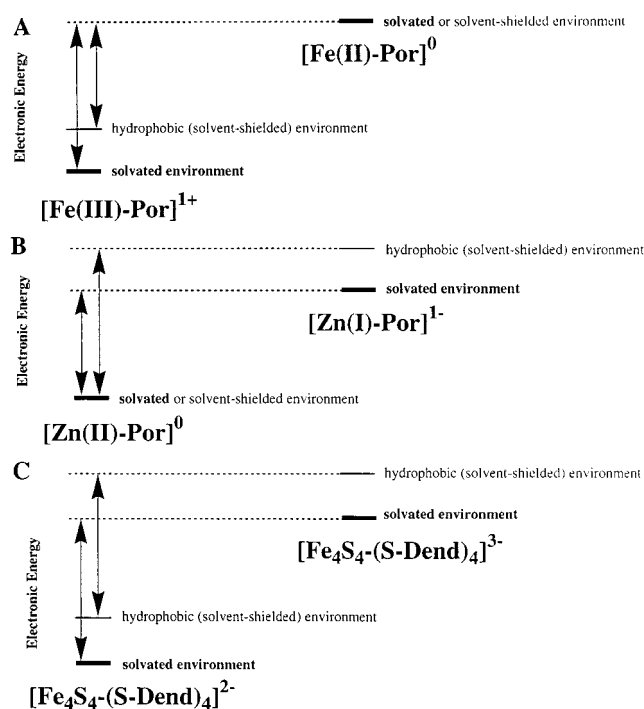
A

$[Fe(II)-Por]^0$ — solvated or solvent-shielded environment

hydrophobic (solvent-shielded) environment

solvated environment

$[Fe(III)-Por]^{1+}$

B

hydrophobic (solvent-shielded) environment

solvated environment

$[Zn(I)-Por]^{1-}$

solvated or solvent-shielded environment

$[Zn(II)-Por]^0$

C

hydrophobic (solvent-shielded) environment

solvated environment

$[Fe_4S_4\text{-}(S\text{-}Dend)_4]^{3-}$

hydrophobic (solvent-shielded) environment

solvated environment

$[Fe_4S_4\text{-}(S\text{-}Dend)_4]^{2-}$

Electronic Energy

FIGURE 1. Model for relative thermodynamic destabilization of *charged* redox states ("charge destabilization") buried inside the hydrophobic dendrimer interior. (A) Model for the one-electron reduction in Fe(III)—porphyrin core dendrimers; (B) model for the one-electron reduction in Zn(II)—porphyrin core dendrimers; and (C) model for the one-electron reduction in [Fe₄S₄] core dendrimers.

Table 1. Reduction Potential ($E_{1/2}$) and Redox Potential Shifts ($\Delta E_{1/2}$) for Metalloporphyrin Core Dendrimers

| structure	solvent	$E_{1/2}$ (mV)	$\Delta E_{1/2}$ (mV)	ref
Zn-TPP	CH_2Cl_2	-1210^a		42
			-10	
1	CH_2Cl_2	-1220^a		42
			-150	
2^b	CH_2Cl_2	-1370^a		42
3	CH_2Cl_2	-210^c		35
			290	
4	CH_2Cl_2	80^c		35
			20	
5	CH_2Cl_2	100^c		35
3	MeCN	-240^c		35
			230	
4	MeCN	-10^c		35
			100	
5	MeCN	90^c		35
3	H_2O	-290^d		35
			40	
4	H_2O	-250^d		35
			340	
5	H_2O	90^e		35

^{a} Potential vs Ag/Ag⁺. ^{b} Higher generation dendrimers showed reductions only as shoulders in the CV and are thus not tabulated here. ^{c} Potential vs SCE. ^{d} Values obtained via equilibrium measurements with $[Fe(ox)_3]^{4-}/Fe(ox)_3]^{3-}$ (ox = oxalate) as reference. ^{e} Value obtained via equilibrium measurements with $[Fe(CN)_6]^{4-}/Fe(CN)_6]^{3-}$ as reference.

cluster.[41] This enables a single type of metal complex to exhibit a wide range of redox potentials in vivo. Structural features within the macromolecular architecture surrounding redox centers affect these properties. To date, these features and their relative influence have not been elucidated with great specificity. Redox-active core dendrimers may be appropriate systems for mimicking a protein microenvironment.[30–40]

In this section, we highlight how dendritic encapsulation influences thermodynamic redox potential in various metallodendrimer architectures from the standpoint of relative solvent accessibility and charge destabilization. These parameters have been cited as critical factors in determining redox potential in metalloproteins. Here, we propose a simple model that rationalizes how redox potential can be influenced in three series of metallodendrimers.

In cytochrome *c*, the redox potential for the one-electron Fe(III) → Fe(II) redox couple is shifted by 300–400 mV compared to the small, solvent-exposed heme models.[41] The shift in redox potential is caused by the hydrophobic protein interior, which destabilizes the charged Fe(III)—porphyrin redox state relative to the neutral Fe(II)—porphyrin redox state. Figure 1A depicts this behavior. Destabilization of the oxidized state by a hydrophobic protein environment lowers the overall energy difference between the oxidized and reduced states, thus facilitating reductive electron transfer from a thermodynamic standpoint. In other words, reduction of the cationic Fe(III)—porphyrin center to the neutral Fe-

(II)—porphyrin center becomes thermodynamically *easier* when the porphyrin is buried inside the hydrophobic protein interior.

The effect of dendrimer hyperbranching on redox potential has been quantified for Zn—porphyrin core dendrimers[42] and for Fe—porphyrin core dendrimers[33,35] with well-defined axial ligation patterns (Table 1). Shifts in reduction potentials of 150 mV (in CH_2Cl_2) for Zn—porphyrin core dendrimers were observed upon increased hyperbranching. More dramatic shifts in redox potential were observed in Fe—porphyrin core dendrimers. In various polar solvents, the redox potential of the Fe—porphyrin core shifted dramatically with increasing amount of hyperbranching, but at different molecular weights depending on the solvent (Table 1). In H_2O, the most significant shift in reduction potential (340 mV) was observed between molecules **4** and **5** (Chart 1). In two organic solvents, the most significant shift in redox potential was between molecules **3** and **4** (290 mV in CH_2Cl_2 and 230 mV in MeCN). Thus, in organic solvent, the degree of hyperbranching in molecule **4** apparently establishes the dendritic microenvironment around the porphyrin. Alternatively, in water, the redox behavior of the porphyrin suggests that it is solvent-exposed in molecule **4**. Perhaps the hydrophilic poly(ethylene glycol) units at the dendrimer periphery facilitate the extensive solvation in water compared to the organic solvents.

On the basis of the above data and the trends observed in redox proteins, solvent accessibility is purported to be the most important factor in controlling redox potential in metallodendrimers. Axially ligated Fe—porphyrin dendrimers (**3–5**) experience changes in redox potential similar to those found in heme proteins, indicating that these structures are viable heme—protein mimics.[30–36,38–40]

Chart 1

3, R =

4, R =

5, R =
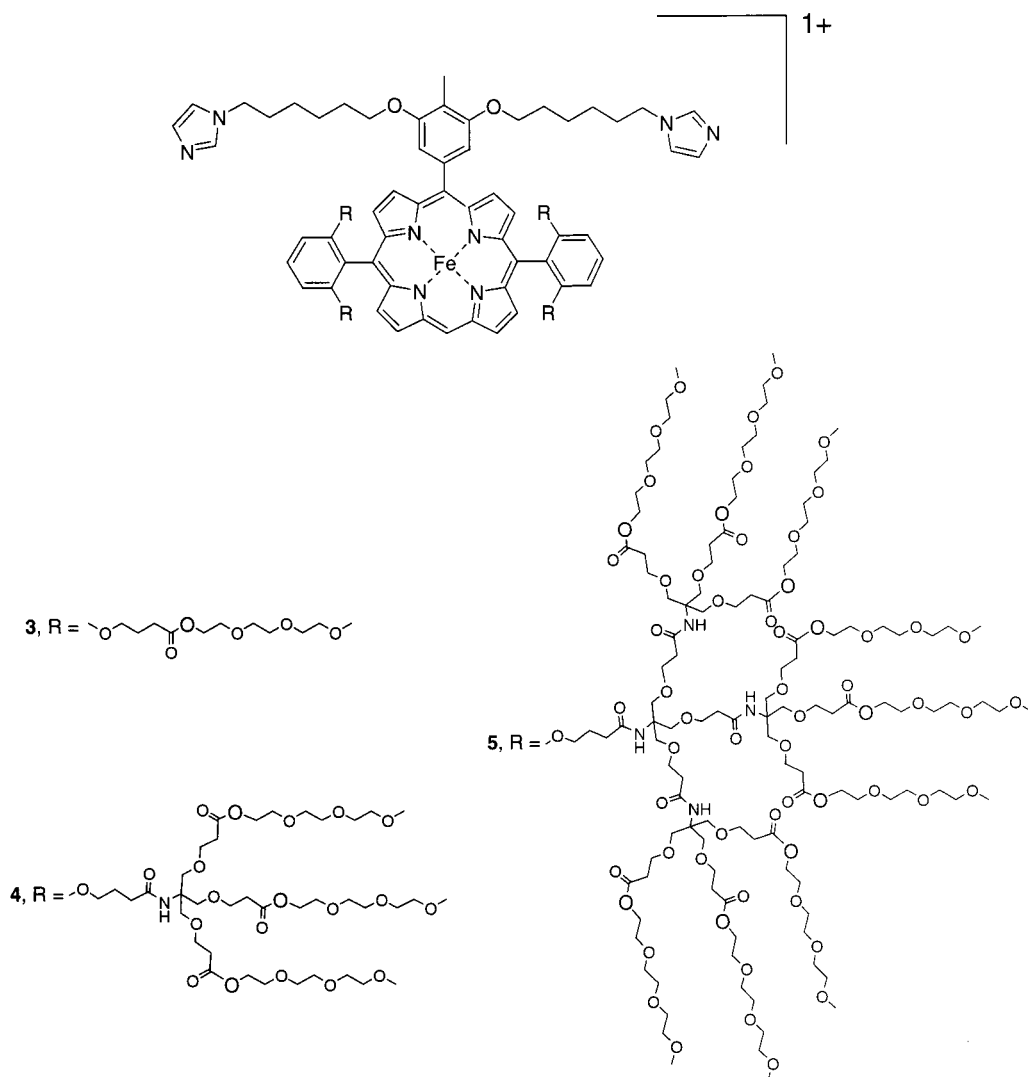
These capped Fe(III)–porphyrin dendrimers exist as the cationic chloride salt. Reduction to the neutral Fe(II)–porphyrin occurred at more *positive* potentials with increasing molecular weight (Table 1). This result indicates that the one-electron reduction becomes *easier* with increasing molecular weight. Although this behavior may not be intuitive (since the electron transfer *rate* decreases with increasing molecular weight), such behavior is consistent with the model in Figure 1A. Thus, the dendrimer architecture apparently mimics the hydrophobic microenvironment inside of heme–proteins.

Solvent accessibility appears to play a role in determining redox potential in Zn–porphyrin core dendrimers as well. A shift to more *negative* potentials was observed for the one-electron reduction in the Zn–porphyrin core dendrimers (**Zn-TPP**, **1**, and **2**) with increasing molecular weight (Table 1).[42] This behavior is opposite of the trend observed for Fe–porphyrin core dendrimers (**3–5**). This disparity is resolved by considering the interactions between the hydrophobic dendrimer interior and the respective redox states. The model depicted in Figure 1B offers a rationale for the shift to negative potentials observed. As the Zn–porphyrin core becomes encapsu-

lated, the charged reduced state is destabilized relative to the neutral oxidized state, thus making the difference in potential between the oxidized and reduced states
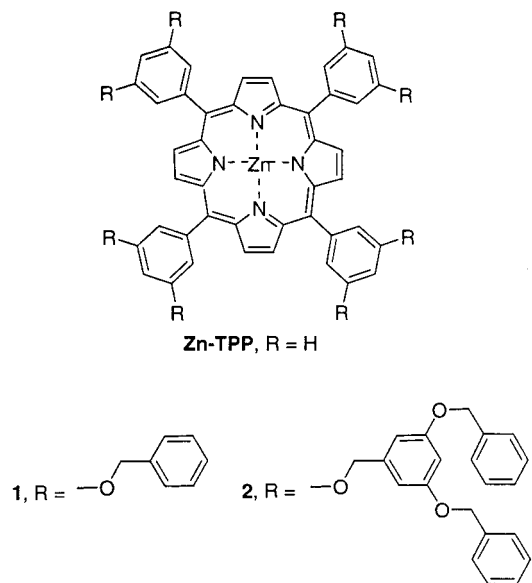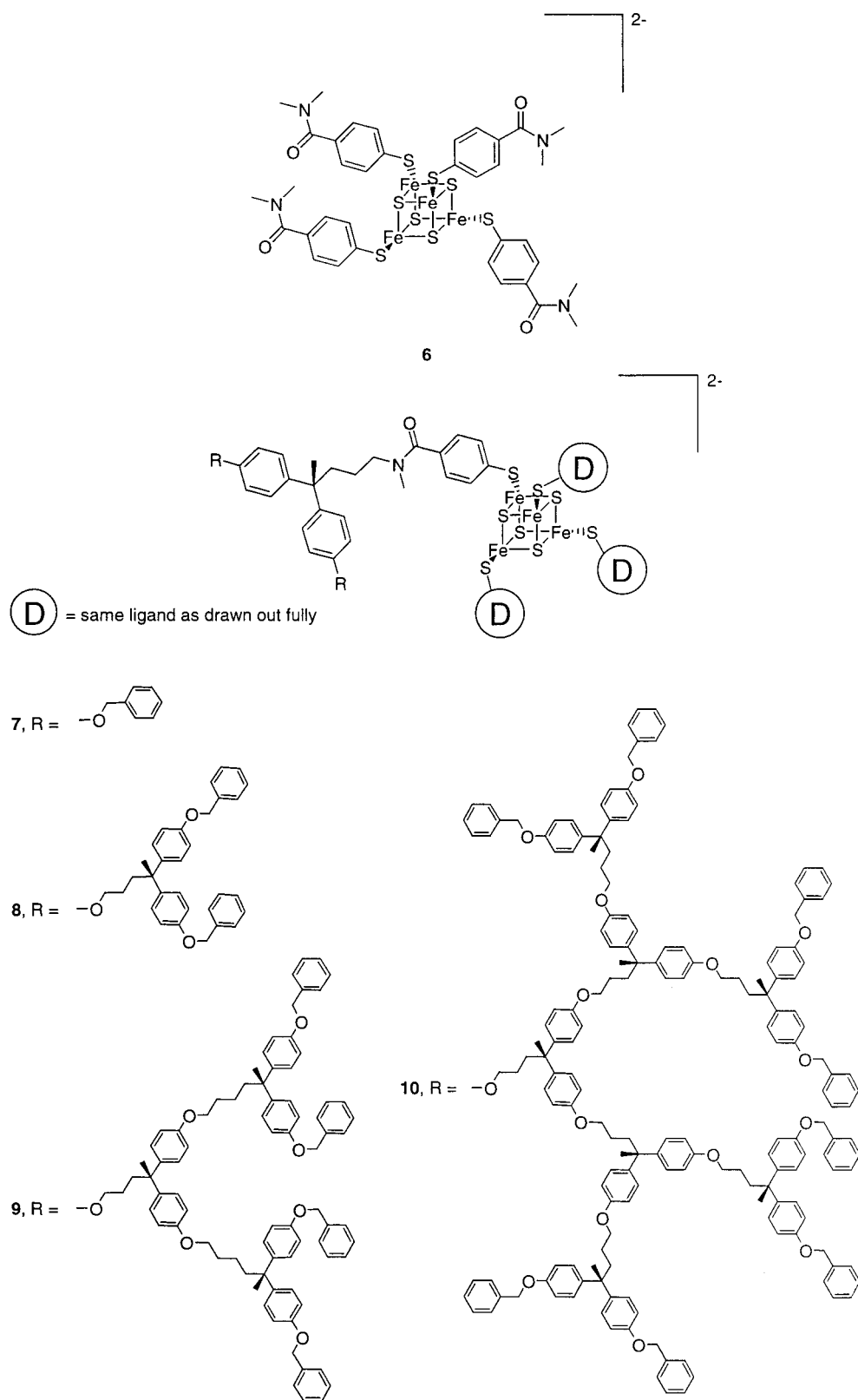

Zn-TPP, R = H

1, R =   **2**, R =

Chart 2

6

$\bigodot_{D}$ = same ligand as drawn out fully

7, R =

8, R =

9, R =

10, R =

larger with increasing encapsulation. The one-electron reduction becomes *harder* as the Zn−porphyrin becomes encapsulated inside a hydrophobic microenvironment (Table 1), as depicted in Figure 1B.

The model illustrated in Figure 1B considers only the change in formal charge of the redox state. Thus, although

it is useful, it is admittedly simplistic. For example, the model predicts significant shifts in oxidation potential as well as reduction potential in the Zn−porphyrin system. On the contrary, the first oxidation potential of molecules **Zn-TPP, 1**, and **2** shows little dependence on dendrimer molecular weight.[42] A more detailed understanding of how

Table 2. Redox Potentials (2−/3−) for [Fe₄S₄] Cluster Compounds[a]

[Fe₄S₄] compound	$E_{1/2}$ (mV)[b]	$E_{1/2}$ (mV)[c]
[Fe₄S₄(CBz-Cys-Ile-Ala-Cys-Gly-Ala-Cys-OMe)(CBz-Cys-Pro-Leu-OMe)]²⁻		−830
[Fe₄S₄(CBz-Cys-Gly-Ala-Cys-OMe)₂]²⁻		−910
[Fe₄S₄(CBz-Cys-Ile-Ala-Cys-OMe)₂]²⁻		−910
[Fe₄S₄(CBz-Cys-Ile-Ala-Cys-Gly-OMe)₂]²⁻		−910
[Fe₄S₄(CBz-Cys-Gly-Ala-OMe)₄]²⁻		−1000
[Fe₄S₄(CBz-Cys-Pro-Ala-OMe)₄]²		−1070
[Fe₄S₄(CBz-Cys-Pro-Leu-OMe)₄]²⁻		−1190
6	−1352	
7	−1360	
8	−1366	
9	−1371	

[a] References 13 and 43. [b] Potential vs Ag/Ag⁺ in DMF. [c] Potential vs SCE in CH₂Cl₂.

the electroactive center is solvated in each redox state is probably necessary here and does not exist at present.

In contrast to the metalloporphyrin core dendrimers, the redox potential of [Fe₄S₄] core dendrimers (**6−9**, Chart 2) is virtually independent of dendrimer molecular weight (Table 2).[13] Why do metalloporphyrin core dendrimers show redox potential shifts and [Fe₄S₄] core dendrimers do not? There are three ways to consider this question.

The first possibility is to consider the factors that influence redox potential in [Fe₄S₄] protein models. The [Fe₄S₄] cluster that is found at the core of molecules **6−10** (Chart 2) is found within the 4-Fe ferrodoxin proteins. As in heme-type proteins, the redox-active [Fe₄S₄] cluster exhibits dramatically different potentials in different protein environments. In one study, [Fe₄S₄] peptide models showed redox potential shifts of 360 mV in response to changes in peptide sequence (Table 2).[43] Since solvent accessibility of the iron−sulfur cluster was assumed to remain constant as the peptide sequence around it was varied, the large changes in redox potential in this series indicated that alternative structural parameters (besides solvent accessibility) were significantly affecting redox potentials in [Fe₄S₄] peptide models. Thus, solvent accessibility may not be the only critical parameter for controlling redox behavior in [Fe₄S₄] cluster compounds, including [Fe₄S₄] core dendrimers.

A second way to rationalize the trends in redox potential in [Fe₄S₄] core dendrimers is to apply the simple model depicted in Figure 1C. In the case of [Fe₄S₄] core dendrimers (**6−10**), the quasi-reversible (2−/3−) redox couple was considered. Both the oxidized state ([Fe₄S₄(S-Dend)₄]²⁻) and the reduced state ([Fe₄S₄(S-Dend)₄]³⁻) are charged, unlike in the cases shown in Figure 1A,B. Therefore, burying the [Fe₄S₄] cluster inside a hydrophobic pocket may destabilize both states to approximately the same relative degree. The energy difference between the oxidized and reduced states would be largely maintained, and no large change in redox potential is predicted using this model (Figure 1C).

A third possible rationale is that, in the [Fe₄S₄] core dendrimers, the dendritic ligands do not intimately encapsulate the redox-active unit in the same way as in the metalloporphyrin dendrimers. The core environment may

be solvated even at high dendrimer generations; thus, no hydrophobic pocket forms around the redox-active unit. There are, after all, potentially very important architectural differences between porphyrin core and [Fe₄S₄] core dendrimers. As will be shown in the following section, architectural differences can lead to very different conformations in model systems. A more complete set of techniques for probing dendrimer conformation and, accordingly, core microenvironment systematically within different dendrimers is necessary to address this possibility and will be a focus of future research.

B. Effect of Dendritic Architecture on Electron-Transfer Rate. Encapsulation of redox-active units influences not only thermodynamic redox potential but also electron-transfer rate in metallo-macromolecules. Controlling electron transfer over large distances has long been a central theme in biological chemistry[44] and has recently emerged in nanoscale electronics schemes.[13,45] Incorporation of dendritic architectures into areas of biomimetic materials and nanoscale electronics requires an understanding of how encapsulation influences the electron-transfer rate. Here we highlight the importance of dendrimer architecture and conformation in electron-transfer rate attenuation.

Every investigation of redox-active core dendrimers by electrochemistry has shown that increasing the degree of hyperbranching in the dendrimer has an effect on the voltammetry consistent with slower electron-transfer kinetics. Using different types of [Fe₄S₄] core dendrimers shown below, we have quantified this effect. Furthermore, we have attempted to relate electron-transfer rate attenuation to the conformation of the dendrimer architecture. As will be indicated below, it is the conformation of the dendrimer, not merely consideration of its primary structure, that governs electron-transfer rate attenuation.

Although little change in the thermodynamics of electron transfer was observed in the series of [Fe₄S₄] core dendrimers, these molecules did exhibit large differences in their rate of electron transfer as measured electrochemically. Specifically, the electron-transfer kinetics for the (2−/3−) redox couple (in DMF) of [Fe₄S₄] core dendrimers were studied. To probe how the electron-transfer rate of the redox-active core was affected by various dendritic architectures, heterogeneous electron-transfer rate constants ($k°$) were determined for molecules **6−10** and molecules **11−13** (Chart 3). The results of these experiments are shown in Table 3. From measured diffusion coefficients, the size of these molecules could be approximated using the Stokes−Einstein equation. Using these techniques and molecular modeling, electron-transfer rate constants were compared from the standpoint of both dendrimer molecular weight and molecular radius (Table 3).[13]

Trends in electron-transfer rate as functions of both molecular weight and dendrimer architecture were observed. Significant electron-transfer rate attenuation was apparent as molecular weight increased for both flexible and rigid [Fe₄S₄] core dendrimers. On a molecular weight
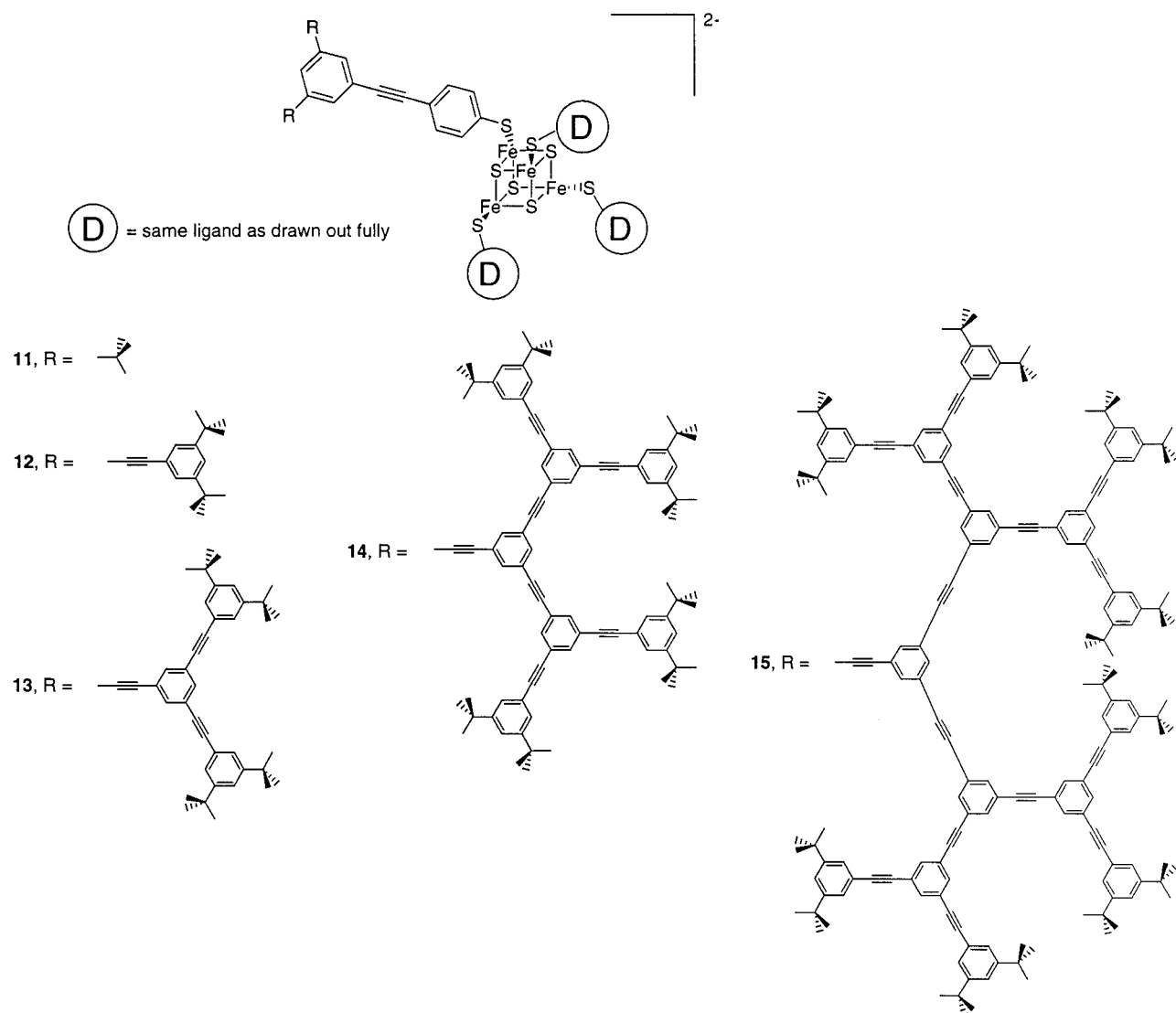
Chart 3

Table 3. Electron Transfer Rate Constants (2−/3−), Hydrodynamic Radii (R_H), and Radius of Gyration (R_g) for [Fe$_4$S$_4$] Core Dendrimers[13]

structure	MW	$k°$ ($\times 10^3$ cm/s)[a]	R_H (Å)[b,c]	R_g (Å)
6	1558	7.43 (1.31)		
7	3240	6.15 (0.64)	7.85 (0.37)	7.75
8	5995	3.29 (0.44)	10.86 (1.94)	10.84
9	11507	0.76 (0.03)	13.49 (4.02)	13.07
10	22529	0.13[d](0.06)	16.92	
11	2121	6.24 (0.59)		
12	3370	4.12 (0.78)	12.56 (3.36)	15.02
13	5867	2.35 (0.09)	14.43 (3.50)	18.70
14	10862			20.89
15	20852			24.84

[a] Values obtained by Osteryoung square wave voltammetry in DMF; values in parentheses represent the magnitude of the 90% confidence intervals of these values. [b] Diffusion coefficients (obtained experimentally from chronoamperometry (DMF)) were used to obtain R_H using the Stokes−Einstein equation. [c] Values in parentheses represent the magnitude of the 90% confidence intervals. [d] Value obtained using an irreversible model.

scale, the rigid architectures (**11−15**, Chart 3) exhibited significantly lower electron-transfer rates than did the flexible architectures (**6−10**). Clearly, there is a confor-

mational difference between these two groups of [Fe$_4$S$_4$] core dendrimers that is important in rationalizing this behavior.[13]

In two-dimensional depictions of dendrimers, the space-filling hyperbranching architecture surrounds a centrally located molecular core. This general physical picture is adequate in a static sense. However, in solution, dendrimers are dynamically fluctuating molecules. A static physical picture does little to describe the range of conformations available for a given architecture in solution. It is this range of conformations that defines how effectively the dendrimer architecture surrounds and thus encapsulates the core. Understanding how the primary chemical structure relates to dendrimer conformation is thus vital in establishing rational design strategies for encapsulation.

To this end, a quenched molecular dynamics technique has been used to assess the range of conformations available in the flexible (**6−10**) versus the rigid (**11−15**) [Fe$_4$S$_4$] core dendrimer models. The most significant structural difference between flexible and rigid [Fe$_4$S$_4$] core
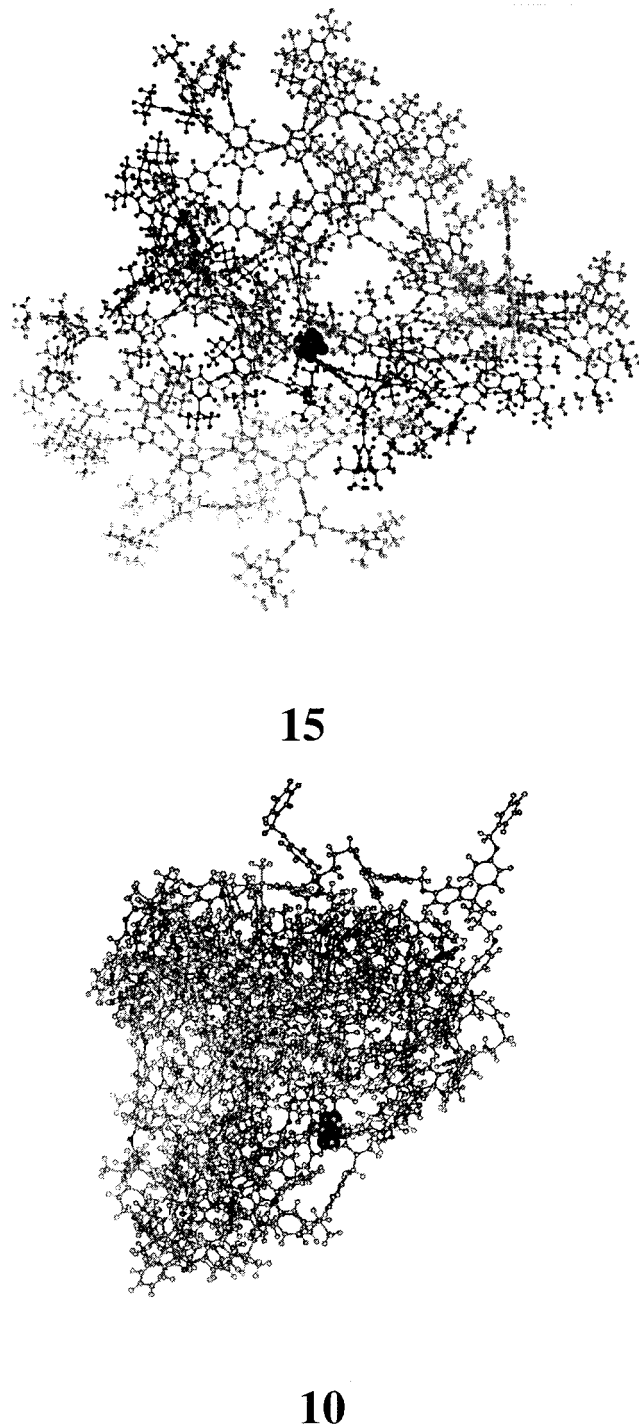
15

10

FIGURE 2. Lowest energy conformer (out of 250 conformers) for models of **10** and **15** generated using a quench molecular dynamics technique.[13]

dendrimer models is the relative positioning of the core. A substantially more offset core was observed in low-energy conformers for the flexible models compared with the rigid models. For example, in ball-and-stick representations of the lowest energy conformations of models of **15** and **10**, the core is observed to be centrally located in the rigid model but virtually at the molecular edge in the flexible model (Figure 2).[13] These data are discussed more in the following section.

Correlation of the results of these simulations with the electron-transfer rate data suggested the possibility that a component of electron transfer in the flexible dendrimers occurs on asymmetric conformers such as those illustrated by the snapshot of a model of **10** in Figure 2. In contrast, in the stiff dendrimers, the redox core is held much more rigidly in the center of the molecule. This observation rationalizes the difference in relative electron-transfer rates between rigid (**11**−**13**) and flexible dendrimers (**6**−**10**). The rigid dendrimers effectively encapsulate the molecular core better than the flexible dendrimers because of this conformational difference between the two types of molecules.[13]

Up to this point, encapsulation has been considered from the standpoint of steric shielding of the core from the electrode surface. Attenuation of electron-transfer rate constants in the rigid $[Fe_4S_4]$ core dendrimers was rationalized by a physical picture in which the rigid dendron ligands serve as a molecular cage around the redox-active unit, effectively separating it from the electrode. Alternatively, one can consider the relative abilities of the dendrimer units to mediate electron transfer *per unit distance.* In the case of dynamically fluctuating molecules in solution, a truly accurate experimental measure of electron-transfer distance is challenging to obtain. However, one might approximate this distance roughly as the dendrimer radius. Using the radius of gyration as effectively an upper limit for the electron transfer distance, it appears that rigid dendrimers pass electrons more efficiently than flexible dendrimers per unit distance. For example, electron transfer in **10** is an order of magnitude slower compared with that in **13**, even though these structures have similar radii of gyration (Table 3). Therefore, from the standpoint of electron mediation per unit distance, the flexible architecture attenuates electron transfer more effectively. This conclusion contrasts earlier conclusions based solely on molecular weight.[13]

C. Encapsulation of Photoactive Dendritic Cores. Other phenomena besides electron-transfer behavior are influenced by encapsulation. This is illustrated in dendritic architectures with photoactive units at the dendritic core. Such molecules show luminescence behaviors that are enhanced upon encapsulation.[8,10,40,42,46−48] These behaviors are potentially useful in schemes for dendritic light harvesting and nanoscale photonic materials and devices.[4−12] Understanding how encapsulation by a dendritic architecture influences quench rate, excited-state lifetimes, and quantum yields is necessary for rational design strategies.

Vögtle et al. incorporated luminescent $[Ru(bpy)_3]^{2+}$ units as dendritic cores coordinated to different types of bipyridine ligands (**L1**−**L7**, Chart 4).[46,47] A variety of dendritic structures were synthesized, and the rate at which dioxygen quenched the $[Ru(bpy)_3]^{2+}$-centered excited state was monitored as a function of dendrimer molecular weight and architecture. For a given molecule to quench an excited state centered at the $[Ru(bpy)_3]^{2+}$ unit, it must penetrate the dendrimer and get within a few angstroms of the dendritic core. Luminescence from the $[Ru(bpy)_3]^{2+}$ core was observed to become more

Chart 4

L1, R = —O—⟨benzyl⟩

L2, R = —O

L3, R = —O

L6, R =

L7, R = —O

L5, R =

L4, R = -OCH₂CH₃
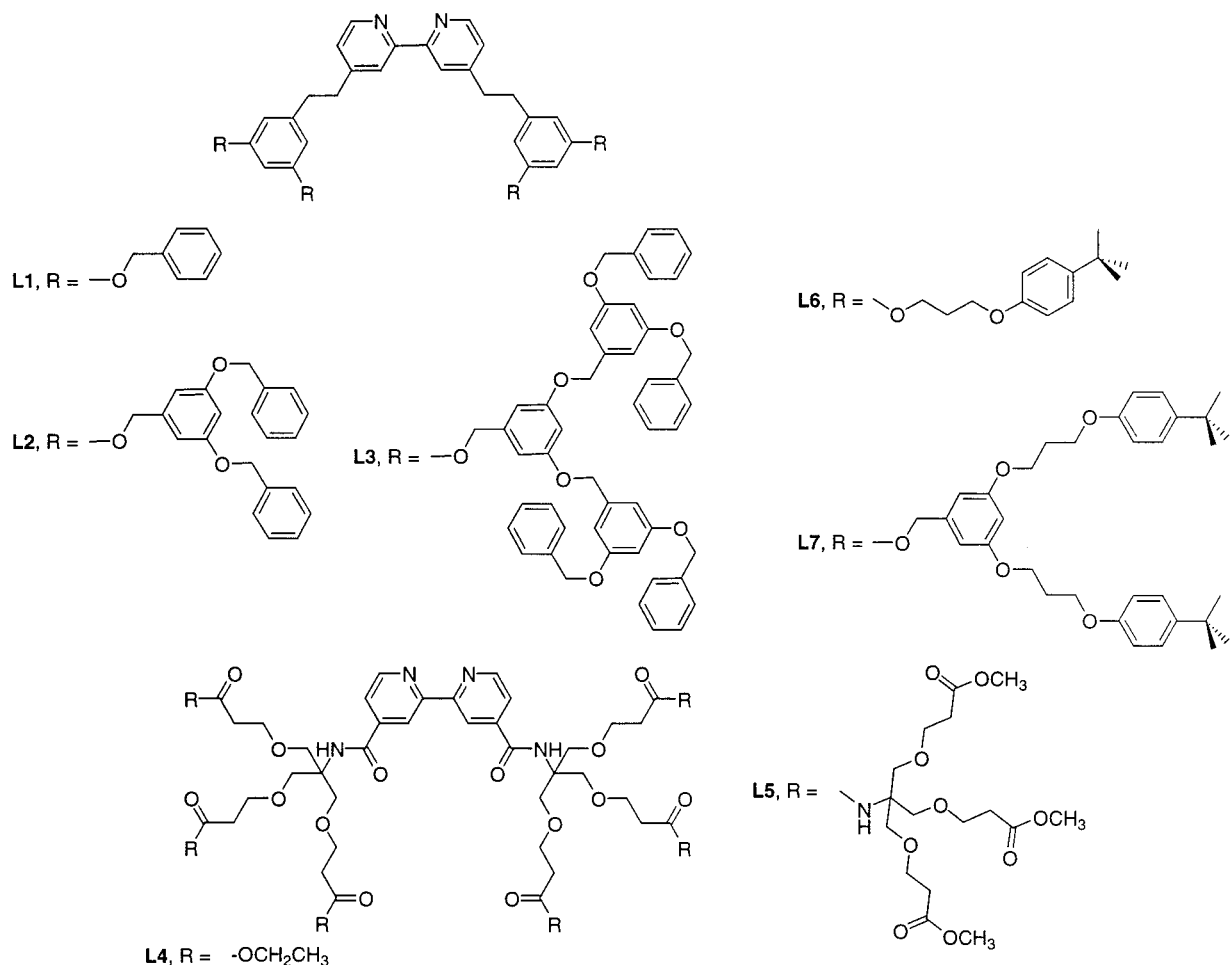
Table 4. Excited-State Quenching Properties for [Ru(bpy)₃]²⁺ Core Dendrimers

structure	MW[a]	$k°_q$ (M⁻¹ s⁻¹)[b]	τ (μs)[c]	ϕ (× 10²)[d]	ref
[Ru(bpy)₃]²⁺	858		0.172	1.6	46
[Ru(**L1**)₃]²⁺	2757		0.191	1.9	46
[Ru(**L2**)₃]²⁺	5304		0.316	2.9	46
[Ru(**L3**)₃]²⁺	10390		0.562	4.8	46
[Ru(bpy)₃]²⁺	858	1.00	0.172	1.6	47
[Ru(**L4**)₃]²⁺	3544	0.17	0.760	7.0	47
[Ru(**L5**)₃]²⁺	9544	0.09	1.010	6.2	47
[Ru(bpy)₃]²⁺	858	1.00	0.172	1.6	46
[Ru(bpy)₂(L6)]²⁺	1674	1.00	0.170	1.8	46
[Ru(bpy)₂(L7)]²⁺	3143	0.67	0.193	1.9	46
[Ru(**L7**)₃]²⁺	7708	0.23	0.415	3.5	46

[a] All molecular weights include two PF₆⁻ counterions. [b] Dioxygen quench rate constant (normalized to [Ru(bpy)₃]²⁺) calculated from the Stern–Volmer equation[47] in aerated MeCN. [c] Lifetime of the luminescent excited state at 298 K. [d] Quantum yield.

efficient as the core became more encapsulated, i.e., shielded from quencher molecules. For example, the rate of excited-state quenching, $k°_q$, was attenuated by a factor of 4 in [Ru(**L7**)₃]²⁺ and by an order of magnitude in [Ru(**L5**)₃]²⁺ compared to [Ru(bpy)₃]²⁺ (Table 4). For most of the molecules studied, attenuation of the $k°_q$ rate constant and increase in lifetime scaled roughly with molecular weight. However, structures [Ru(**L4**)₃]²⁺ and [Ru(bpy)₂-(**L7**)]²⁺ exhibited $k°_q$ values that differ by a factor of 4, despite similar molecular weights. In this case, the type

of dendrimer structure employed and the symmetry of its distribution around the core lead to differences in encapsulation behavior.

III. Elucidation of Dendrimer Conformation

Rational design strategies for dendritic encapsulation must rely on some understanding of how chemical structure influences dendrimer conformation. It is the aim of this section to illustrate how conformational flexibility in dendrimers is important in rationalizing electron-transfer and luminescence behaviors. Both experiment and computation have been employed to study dendrimer conformation and conformational flexibility.

Early on, several approaches emerged for investigating dendrimer conformation. Molecular dynamics simulations on atomistic models of PAMAM dendrimers showed steric congestion at a critical molecular weight.[3] This particular simulation represented an extremely short experimental time scale but was augmented by NMR data that also showed a transition from an open, extended to a compact structure with increasing molecular weight. Other computations were performed on more simplistic coarse-grain "ball-and-stick" models.[49–56] These computations indicated branch ends distributed throughout the molecule and, in some cases, a density maximum at the center of

the molecule.[57] Several experiments have been performed to elucidate features of dendrimer conformation using NMR,[3,40,58−61] solvatochromism[1,62,63] and intrinsic viscosity.[2] Although a full elucidation of the techniques, molecules, observations, and conclusions is beyond the scope of this Account, in general these investigations of dendrimer conformation were consistent with the trends found in computational investigations. Most of these experiments revealed qualitative features of conformation, with the exception of solid-state rotational-echo double-resonance (REDOR) NMR on nuclear-labeled dendrons performed by Wooley et al.[60] In this work, an average intramolecular distance of 12 Å between focal and peripheral units was determined for generations 3, 4, and 5. These results in particular indicate quantitatively inward folding of chain ends (also termed "back-folding" in other literature).[64,65] Using these data to establish distance constraints, subsequent molecular dynamics simulations on a generation 5 dendrimer model rendered structures with densely packed interior regions.

The obvious next step was to ask which chemical repeat units were most efficient specifically for dendritic encapsulation strategies. Until recently, few modeling studies of dendrimers incorporated atomistic detail, a critical element for mapping out molecular structure−property relationships. A first effort on our part[66] employed a high-temperature dynamics/simulated annealing protocol on alternatively flexible and stiff dendrimers based on repeat units reported by Moore et al.[67,68] and Fréchet et al.[69,70] This procedure was performed to ensure geometric equilibration of the models. Flexible-unit dendrimers were found to be globular and much closer to spherical in shape compared to stiff-unit dendrimers, which were more disklike in shape.

Interestingly, in all of the types of dendrimers studied, the different generations within each molecule were found to be radially distributed throughout the interior. In the case of flexible dendrimers, this behavior was attributed to back-folding of some of the repeat units that have low-energy torsional potentials (they can kink easily). However, it was less intuitive as to why this same type of distribution was observed in stiff-chain dendrimers as these cannot back-fold in the same way (they cannot kink). The distribution comes from the very nature of hyperbranching: at every hyperbranch, the dendrimer "turns" as it grows outward, leading to pathways which "turn in" as well as "turn out" (Figure 3). Thus, this geometry affords radially scattered repeat units even for conformationally stiff architectures.

Along with computational efforts, we also addressed the question of dendrimer conformation experimentally.[71] In section II.B, encapsulation in $[Fe_4S_4]$ core dendrimers was discussed. These dendrimers have a paramagnetic inorganic cluster at their topological center, and this paramagnetic core can influence the relaxation time of the nuclei in the surrounding architecture. This feature was used to probe dendrimer conformation. The relaxation time constants for **9** were compared to a diamagnetic analogue in which the $[Fe_4S_4]$ core was replaced with
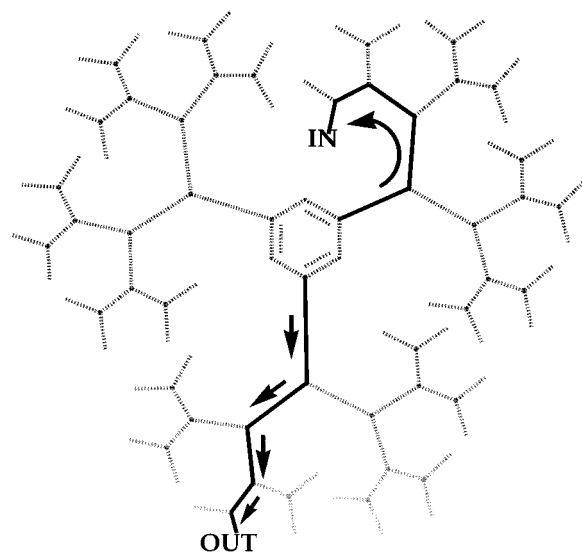

FIGURE 3. Generic representation of a "rigid" dendritic architecture (i.e., no mechanism for back-folding by bending or kinking). Two pathways are indicated: one that "turns in", labeled IN, at the terminus and one that "turns out", labeled OUT, at the terminus.

a tetraphenyl methane core. Lowering of relaxation time constants for nuclei throughout all parts of the dendrimer architecture indicated that, on the time scale of the NMR experiment, some of each group of chemical-shift-equivalent nuclei penetrate the local vicinity of the inorganic cluster (Figure 4). Such a picture contrasts one in which the dendron arms remain radially extended on the time scale of the NMR experiment.

This picture was supported by simulated annealing molecular dynamics simulations performed on a model of **9**. Radial distribution functions (Figure 5A)[71] showed that some of the nuclei in each generation of the dendrimer come into close proximity with the core. In addition, analysis of mean-square displacement correlation functions on each set of nuclei showed a substantially more mobile set of terminal groups compared to all the internal repeat units (Figure 5B).[71] This behavior is consistent with the larger $T1$ values obtained for these nuclei compared to their internal counterparts and likely reflects the difference in coordination number between the internal units of the dendrimer and its "fingertips".

Computational modeling was also employed to rationalize trends in electron-transfer rate attenuation in flexible and rigid $[Fe_4S_4]$ core dendrimers. A conformational searching technique based on high-temperature molecular dynamics was employed to sample a range of dendrimer conformations. The conformational searching protocol was adapted from a protocol used on polypeptides: high-temperature molecular dynamics produced a trajectory from which structures are extracted at regular intervals and rigorously minimized or "cooled".[72−74] Data sets of 250 minimized structures were obtained routinely in 2−3 days (using supercomputing resources). Histogram plots were useful in illustrating the distribution of conformers within a data set, showing likely dendrimer conformations as well as a dynamic range of conformations. Figure 6 shows such a data set obtained for models
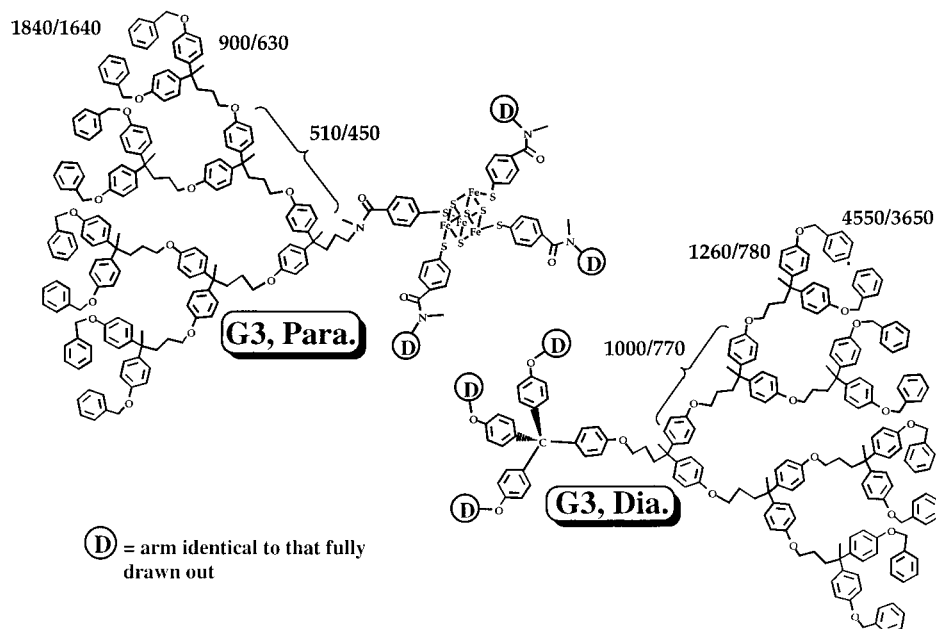
FIGURE 4. Comparison of the $T1$ time constants (ms) for relaxation of chemical shift equivalent protons in a paramagnetic and analogous diamagnetic dendrimer. Reprinted with permission from ref 14. Copyright 1998 Wiley-VCH.
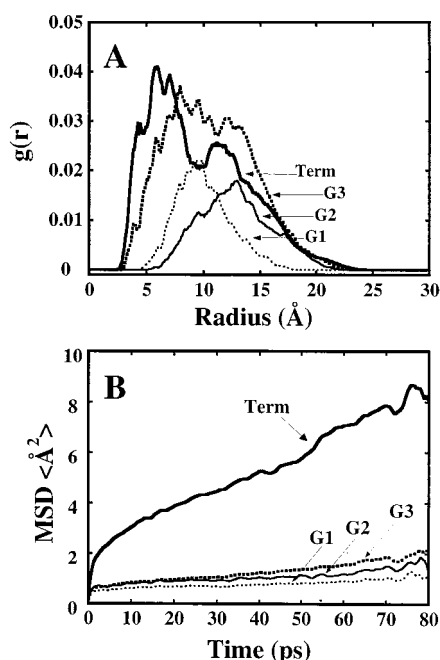

FIGURE 5. (A) Radial density distribution functions for atoms in each generation (Gn = generation n, Term = terminal groups) within an equilibrated model of **9**, showing that repeat units within all the generations contribute to the atom density within 10 Å around the core (located at 0 Å in this plot). (B) Mean square displacement autocorrelation functions for sets of atoms within each generation of model of **9** during the last 80 ps of a molecular dynamics simulation, indicating the relative segmental motion within each of the groups. Reprinted with permission from ref 71. Copyright 1998 American Chemical Society.

of **8** and **13**; qualitatively similar data sets were obtained for the other generations of dendrimers.

From these data, it was concluded that the most important conformational feature from the standpoint of core encapsulation was the relative position of the core
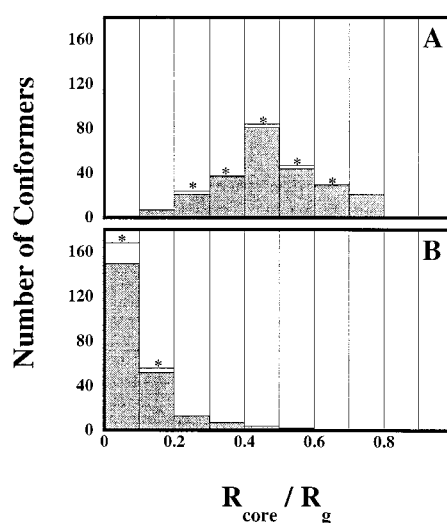

FIGURE 6. Relative core offsets (R_{core}/R_g) from conformational search data sets for models of (A) **8** and (B) **13**. White bars indicate the number of conformers within 10 kcal/mol of the lowest energy conformer. Bins containing any of this set of conformers are marked with an asterisk. Reprinted with permission from the Supporting Information of ref 13. Copyright 1999 American Chemical Society.

within the dendrimer interior. Figure 6 shows that the relative core offset from the center of mass of the molecule (R_{core}/R_g) varied dramatically between rigid and flexible dendrimer architectures. This offset indicates quantitatively how far the core is displaced from the molecular center of mass. The obvious conclusion from this analysis is that offset cores are less encapsulated by the surrounding architecture than are more centrally located cores. For a model of **13**, structures have 0−20% relative core offset, but for a model of **8**, they have a 20−80% offset. In addition, for the model of **8**, a wider range of geometrically different conformations is found compared to the model

of **13**, suggesting a greater mobility in the former compared to the latter. These calculations suggest that flexible architectures have a more mobile and less sterically shielded redox-active core compared to the rigid architectures.

IV. Conclusions

Many different types of dendrimers exhibit common structural features such as back-folding due to hyperbranching, distribution of repeat units throughout the architecture, a dense interior, etc. These generic features are extremely helpful when assessing the viability of a hyperbranched structure in a particular application. However, as shown in this Account, there are important differences between different dendrimer structures: a richer structure−property relationship exists than is uncovered by these simple ideas of dendrimer conformation. Particularly illustrated here is how encapsulation varies with conformational flexibility

Moreover, it was a goal of this Account to show the importance of considering the dynamic behavior of dendrimers when evaluating their properties. Conformational mobility (or, alternatively, shape persistency)[75−77] is not particularly easy to probe experimentally or computationally. However, as illustrated above, computational conformational searching can be brought to bear on this question, and it has been helpful in rationalizing experimental observations. Ultimately, the ideal rational design strategy would always incorporate a dynamic picture of a dendrimer.

Although encapsulation, the way we and others have explored it, is only a behavior and not an application, the ability to tune dendrimer properties with chemical structure suggests that these molecules are amenable to eventual application. With regard to encapsulation, particularly as defined here, we envision dendrimers playing an important role in molecular electronics, luminescent devices, and energy transduction. Surely, rational design and pursuit of application will continue to find a strong synergy in dendrimer science.

References

(1) Devadoss, C.; Bharathi, P.; Moore, J. S. Anomalous shift in the fluorescence spectra of a high-generation dendrimer in nonpolar solvents. *Angew. Chem., Int. Ed. Engl.* **1997**, *36*, 1633−1635.

(2) Hawker, C. J.; Farrington, P. J.; Mackay, M. E.; Wooley, K. L.; Frechet, J. M. J. Molecular ball-bearings—the unusual melt viscosity behavior of dendritic macromolecules. *J. Am. Chem. Soc.* **1995**, *117*, 4409−4410.

(3) Naylor, A. M.; Goddard, W. A., III; Kiefer, G. E.; Tomalia, D. A. Starburst Dendrimers. 5. Molecular Shape Control. *J. Am. Chem. Soc.* **1989**, *111*, 2339−2341.

(4) Adronov, A.; Gilat, S. L.; Frechet, J. M. J.; Ohta, K.; Neuwahl, F. V. R.; Fleming, G. R. Light harvesting and energy transfer in laser-dye-labeled poly(aryl ether) dendrimers. *J. Am. Chem. Soc.* **2000**, *122*, 1175−1185.

(5) Balzani, V.; Campagna, S.; Denti, G.; Juris, A.; Serroni, S.; Venturi, M. Harvesting sunlight by artificial supramolecular antennae. *Solar Energy Mater. Solar Cells* **1995**, *38*, 159−173.

(6) Bar-Haim, A.; Klafter, J.; Kopelman, R. Dendrimers as controlled artificial energy antenna. *J. Am. Chem. Soc.* **1997**, *119*, 6197−6198.

(7) Elicker, T. S.; Evans, D. G. Electron dynamics in dendrimers. *J. Phys. Chem. A* **1999**, *103*, 9423−9431.

(8) Kawa, M.; Frechet, J. M. J. Self-assembled lanthanide cored dendrimer complexes: Enhancement of the luminescence properties of lanthanide ions through site-isolation and antenna effects. *Chem. Mater.* **1998**, *10*, 286−296.

(9) Kopelman, R.; Shortreed, M. R.; Shi, Z.-Y.; Tan, W.; Xu, Z.; Moore, J. S.; Bar-Haim, A.; Klafter, J. Spectroscopic Evidence for Excitonic Localization in Fractal Antenna Supermolecules. *Phys. Rev. Lett.* **1997**, *78*, 1239−1242.

(10) Sato, T.; Jiang, D. L.; Aida, T. A blue-luminescent dendritic rod: Poly(phenyleneethynylene) within a light-harvesting dendritic envelope. *J. Am. Chem. Soc.* **1999**, *121*, 10658−10659.

(11) Shortreed, M. R.; Swallen, S. F.; Shi, Z.-Y.; Tan, W.; Xu, Z.; Devadoss, C.; Moore, J. S.; Kopelman, R. Directed Energy Transfer Funnels in Dendrimeric Antenna Supermolecules. *J. Phys. Chem. B* **1997**, *101*, 6318−6322.

(12) Stewart, G. M.; Fox, M. A. Chromophore-Labeled Dendrons as Light Harvesting Antennae. *J. Am. Chem. Soc.* **1996**, *118*, 4354−4360.

(13) Gorman, C. B.; Smith, J. C.; Hager, M. W.; Parkhurst, B. L.; Sierzputowska-Gracz, H.; Haney, C. A. Molecular structure−property relationships for electron-transfer rate attenuation in redox-active core dendrimers. *J. Am. Chem. Soc.* **1999**, *121*, 9958−9966.

(14) Gorman, C. B. Encapsulated Electroactive Molecules. *Adv. Mater.* **1997**, *9*, 1117−1119.

(15) Jansen, J.; de Brabander-van den Berg, E. M.; Meijer, E. W. Encapsulation of guest molecules into a dendritic box. *Science* **1994**, *266*, 1226−1229.

(16) Jansen, J.; Meijer, E. W.; de Brabander-van den Berg, E. M. The dendritic box—shape-selective liberation of encapsulated guests. *J. Am. Chem. Soc.* **1995**, *117*, 4417−4418.

(17) Jansen, J.; Janssen, R. A. J.; de Brabander-van den Berg, E. M.; Meijer, E. W. Triplet radical pairs of 3-carboxyproxyl encapsulated in a dendritic box. *Adv. Mater.* **1995**, *7*, 561−564.

(18) Brunner, H. Dendrizymes—expanded ligands for enantioselective catalysis. *J. Organomet. Chem.* **1995**, *500*, 39−46.

(19) Naidoo, K. J.; Hughes, S. J.; Moss, J. R. Computational investigations into the potential use of poly(benzyl phenyl ether) dendrimers as supports for organometallic catalysts. *Macromolecules* **1999**, *32*, 331−341.

(20) Piotti, M. E.; Rivera, F.; Bond, R.; Hawker, C. J.; Frechet, J. M. J. Synthesis and catalytic activity of unimolecular dendritic reverse micelles with .internal functional groups. *J. Am. Chem. Soc.* **1999**, *121*, 9471−9472.

(21) Oosterom, G. E.; van Haaren, R. J.; Reek, J. N. H.; Kamer, P. C. J.; van Leeuwen, P. Catalysis in the core of a carbosilane dendrimer. *Chem. Commun.* **1999**, 1119−1120.

(22) Kleij, A. W.; Gossage, R. A.; Jastrzebski, J.; Boersma, J.; van Koten, G. The 'dendritic effect' in homogeneous catalysis with carbosilane-supported arylnickel(II) catalysts: Observation of active-site proximity effects in atom-transfer radical addition. *Angew. Chem., Int. Ed.* **2000**, *39*, 176−178.

(23) Hovestad, N.; Eggeling, E.; Heidbuchel, H.; Jastrzebski, J.; Kragl, U.; Keim, W.; Vogt, D.; van Koten, G. Selective Hydrovinylation of Styrene in a Membrane Reactor: Use of Carbosilane Dendrimers with Hemilabile P,O Ligands. *Angew. Chem., Int. Ed.* **1999**, *38*, 1655−1658.

(24) Gossage, R. A.; Jastrzebski, J.; van Ameijde, J.; Mulders, S.; Brouwer, A.; Liskamp, R.; van Koten, G. Synthesis and Catalytic Application of Amino Acid Based Dendritic Macromolecules. *Tetrahedron Lett.* **1999**, *40*, 1413−1416.

(25) Liu, M. J.; Kono, K.; Frechet, J. M. J. Water-soluble dendrimer−poly(ethylene glycol) starlike conjugates as potential drug carriers. *J. Polym. Sci. Polym. Chem.* **1999**, *37*, 3492−3503.

(26) Pistolis, G.; Malliaris, A.; Tsiourvas, D.; Paleos, C. M. Poly-(propyleneimine) dendrimers as pH-sensitive controlled-release systems. *Chem.-Eur. J.* **1999**, *5*, 1440−1444.

(27) Twyman, L. J.; Beezer, A. E.; Esfand, R.; Hardy, M. J.; Mitchell, J. C. The synthesis of water soluble dendrimers, and their application as possible drug delivery systems. *Tetrahedron Lett.* **1999**, *40*, 1743−1746.

(28) Yoo, H.; Sazani, P.; Juliano, R. L. PAMAM dendrimers as delivery agents for antisense oligonucleotides. *Pharm. Res.* **1999**, *16*, 1799−1804.

(29) Zimmerman, S. C.; Wang, Y.; Bharathi, P.; Moore, J. S. Analysis of amidinium guest complexation by comparison of two classes of dendrimer hosts containing a hydrogen bonding unit at the core. *J. Am. Chem. Soc.* **1998**, *120*, 2172−2173.

(30) Smith, D. K.; Diederich, F. Functional dendrimers: Unique biological mimics. *Chem.-Eur. J.* **1998**, *4*, 1353.

(31) Mattei, S.; Wallimann, P.; Kenda, B.; Amrein, W.; Diederich, F. Dendrophanes: Water-soluble dendritic receptors as models for buried recognition sites in globular proteins. *Helv. Chim. Acta* **1997**, *80*, 2391−2417.

(32) Dandliker, P. J.; Diederich, F.; Zingg, A.; Gisselbrecht, J. P.; Gross, M.; Louati, A.; Sanford, E. Dendrimers with porphyrin cores: Synthetic models for globular heme proteins. *Helv. Chim. Acta* **1997**, *80*, 1773.

(33) Dandliker, P. J.; Diederich, F.; Gisselbrecht, J. P.; Louati, A.; Gross, M. Water-soluble dendritic iron porphyrins: Synthetic models of globular heme proteins. *Angew. Chem., Int. Ed. Engl.* **1996**, *34*, 2725.

(34) Dandliker, P. J.; Diederich, F.; Gross, M.; Knobler, C. B.; Louati, A.; Sanford, E. M. Dendritic Porphyrins−Modulating Redox Potentials Of Electroactive Chromophores With Pendant Multifunctionality. *Angew. Chem., Int. Ed. Engl.* **1994**, *33*, 1739.

(35) Weyermann, P.; Gisselbrecht, J. P.; Boudon, C.; Diederich, F.; Gross, M. Dendritic iron porphyrins with tethered axial ligands: New model compounds for cytochromes. *Angew. Chem., Int. Ed.* **1999**, *38*, 3215.

(36) Collman, J. P.; Fu, L.; Zingg, A.; Diederich, F. Dioxygen and carbon monoxide binding in dendritic iron(II) porphyrins. *Chem. Commun.* **1997**, 193−194.

(37) Enomoto, M.; Aida, T. Self-assembly of a copper-ligating dendrimer that provides a new non-heme metalloprotein mimic: "Dendrimer effects" on stability of the bis(mu-oxo)dicopper(III) core. *J. Am. Chem. Soc.* **1999**, *121*, 874−875.

(38) Jiang, D.-L.; Aida, T. A dendritic iron porphyrin as a novel haemoprotein mimic: effects of the dendrimer cage on dioxygen-binding activity. *Chem. Commun.* **1996**, 1523−1524.

(39) Jin, R. H.; Aida, T.; Inoue, S. "Caged" Porphyrin: the First Dendritic Molecule having a Core Photochemical Functionality. *J. Chem. Soc., Chem. Commun.* **1993**, 1261−1263.

(40) Tomoyose, Y.; Jiang, D.-L.; Jin, R.-H.; Aida, T.; Yamashita, T.; Horie, K.; Yashima, E.; Okamoto, Y. Aryl Ether Dendrimers with an Interior Metalloporphyrin Functionality as a Spectroscopic Probe: Interpenetrating Interaction with Dendritic Imidazoles. *Macromolecules* **1996**, *29*, 5236−5238.

(41) Moore, G. R.; Pettigrew, G. W. *Cytochromes-c: Evolutionary, Structural and Physicochemical Aspects*; Springer: Berlin, 1990.

(42) Pollak, K. W.; Leon, J. W.; Frechet, J. M. J.; Maskus, M.; Abruna, H. D. Effects of dendrimer generation on site isolation of core moieties: Electrochemical and fluorescence quenching studies with metalloporphyrin core dendrimers. *Chem. Mater.* **1998**, *10*, 30−38.

(43) Nakamura, A.; Ueyama, N. Importance of Peptide Sequence in Electron-Transfer Reactions of Iron-Sulfur Clusters. In *Metal Clusters in Proteins*; Que, L., Jr., Ed.; American Chemical Society: Washington, DC, 1988; Vol. 372, pp 293−301.

(44) Elena, B.; Ivano, B.; Marco, B.; Claudio, L.; Xiaoyu, Z.; Igor, V. K.; Adrian, P.; Angel, J. D. B.; Harry, B. G. Bond Mediated Electron Tunneling in Ruthenium Modified High Potential Iron Sulfur Protein. *J. Am. Chem. Soc.* **2000**, *122*, 4532−4533.

(45) Cardona, C. M.; Kaifer, A. E. Asymmetric Redox-Active Dendrimers Containing a Ferrocene Subunit. Preparation, Characterization, and Electrochemistry. *J. Am. Chem. Soc.* **1998**, *120*, 4023−4024.

(46) Vögtle, F.; Plevoets, M.; Nieger, M.; Azzellini, G. C.; Credi, A.; De Cola, L.; De Marchis, V.; Venturi, M.; Balzani, V. Dendrimers with a photoactive and redox-active [Ru(bpy)(3)](2+)-type core: Photophysical properties, electrochemical behavior, and excited-state electron-transfer reactions. *J. Am. Chem. Soc.* **1999**, *121*, 6290−6298.

(47) Issberner, J.; Vogtle, F.; DeCola, L.; Balzani, V. Dendritic bipyridine ligands and their tris(bipyridine)ruthenium(II) chelates−Syntheses, absorption spectra, and photophysical properties. *Chem.-Eur. J.* **1997**, *3*, 706−712.

(48) Jiang, D. L.; Aida, T. Morphology-dependent photochemical events in aryl ether dendrimer porphyrins: Cooperation of dendron subunits for singlet energy transduction. *J. Am. Chem. Soc.* **1998**, *120*, 10895−10901.

(49) Lescanec, R. L.; Muthukumar, M. Configurational characteristics and scaling behavior of starburst molecules: A computational study. *Macromolecules* **1990**, *23*, 2280−2288.

(50) Murat, M.; Grest, G. S. Molecular Dynamics Study of Dendrimer Molecules in Solvents of Varying Quality. *Macromolecules* **1996**, *29*, 1278−1285.

(51) Mansfield, M. L.; Klushin, L. I. Intrinsic Viscosity of Model Starburst Dendrimers. *J. Phys. Chem.* **1992**, *96*, 3994−3998.

(52) Mansfield, M. L.; Klushin, L. I. Monte Carlo Studies of Dendrimer Macromolecules. *Macromolecules* **1993**, *26*, 4262−4268.

(53) Carl, W. A Monte Carlo study of model dendrimers. *J. Chem. Soc., Faraday Trans.* **1996**, *92*, 4151−4154.

(54) Cai, C.; Chen, Z. Y. Rouse Dynamics of a Dendrimer Model in the Θ Condition. *Macromolecules* **1997**, *30*, 5104−5117.

(55) Chen, Z. Y.; Cui, S.-M. Monte Carlo Simulations of Star-Burst Dendrimers. *Macromolecules* **1996**, *29*, 7943−7952.

(56) Boris, D.; Rubinstein, M. A self-consistent mean field model of a starburst dendrimer: Dense core versus dense shell. *Macromolecules* **1996**, *29*, 7251−7260.

(57) This density maximum at the molecular center differed from an earlier prediction by de Gennes, in which dendron arms radiated out from the center causing a radial density gradient, heaviest at the molecular periphery: DeGennes, P. G.; Hervet, H. Statistics of Starburst Polymers. *J. Phys. Lett.* **1983**, *44*, L351-L360.

(58) Meltzer, A. D.; Tirrell, D. A.; Jones, A. A.; Inglefield, P. T.; Hedstrand, D. M.; Tomalia, D. A. Chain Dynamics in Poly(amido amine) Dendrimers. A Study of ^{13}C NMR Relaxation Parameters. *Macromolecules* **1992**, *25*, 4541−4548.

(59) Meltzer, A. D.; Tirrell, D. A.; Jones, A. A.; Inglefield, P. T. Chain Dynamics in Poly(amido amine) Dendrimers. A Study of ^2H NMR Relaxation Parameters. *Macromolecules* **1992**, *25*, 4549−4552.

(60) Wooley, K. L.; Klug, C. A.; Tasaki, K.; Schaefer, J. Shapes of Dendrimers from Rotational-Echo Double-Resonance NMR. *J. Am. Chem. Soc.* **1997**, *119*, 53−58.

(61) Jiang, D.-L.; Aida, T. Photoisomerization in dendrimers by harvesting of low-energy photons. *Nature* **1997**, *388*, 454−456.

(62) Smith, D. K.; Muller, L. Dendritic biomimicry: microenvironmental effects on tryptophan fluorescence. *Chem. Commun.* **1999**, 1915−1916.

(63) Hawker, C. J.; Wooley, K. L.; Fréchet, J. M. J. Solvatochromism as a Probe of the Microenvironment in Dendritic Polyethers: Transition from an Extended to a Globular Structure. *J. Am. Chem. Soc.* **1993**, *115*, 4375−4376.

(64) Bosman, A. W.; Bruining, M. J.; Kooijman, H.; Spek, A. L.; Janssen, R. A. J.; Meijer, E. W. Concerning the Localization of End Groups in Dendrimers. *J. Am. Chem. Soc.* **1998**, *120*, 8547−8548.

(65) Bosman, A. W.; Jannsen, H. M.; Meijer, E. W. About Dendrimers: Structure, Physical Properties and Applications. *Chem. Rev.* **1999**, *99*, 1665−1688.

(66) Gorman, C. B.; Smith, J. C. Effect of Repeat Unit Flexibility on Dendrimer Conformation as Studied by Atomistic Molecular Dynamics Simulations. *Polymer* **2000**, *41*, 675−683.

(67) Xu, Z.; Moore, J. S. Synthesis and Characterization of a High Molecular Weight Stiff Dendrimer. *Angew. Chem., Int. Ed. Engl.* **1993**, *32*, 246−248.

(68) Xu, Z.; Kahr, M.; Walker, K. L.; Wilkins, C. L.; Moore, J. S. Phenylacetylene Dendrimers by the Divergent, Convergent, and Double-Stage Convergent Methods. *J. Am. Chem. Soc.* **1994**, *116*, 4537−4550.

(69) Hawker, C. J.; Fréchet, J. M. J. Preparation of Polymers with Controlled Molecular Architecture. A New Convergent Approach to Dendritic Macromolecules. *J. Am. Chem. Soc.* **1990**, *112*, 7638−7647.

(70) Wooley, K. L.; Hawker, C. J.; Fréchet, J. M. J. Hyperbranched Macromolecules via a Novel Double-Stage Convergent Growth Approach. *J. Am. Chem. Soc.* **1991**, *113*, 4252−4261.

(71) Gorman, C. B.; Hager, M. W.; Parkhurst, B. L.; Smith, J. C. Use of a paramagnetic core to affect longitudinal nuclear relaxation in dendrimers−a tool for probing dendrimer conformation. *Macromolecules* **1998**, *31*, 815−822.

(72) Sun, Y.; Kollman, P. A. Conformational Sampling and Ensemble Generation by Molecular Dynamics Simulations: 18-Crown-6 as a test Case. *J. Comput. Chem.* **1992**, *13*, 33−40.

(73) Al-Obeidi, F.; O'Connor, S.; Job, C.; Hruby, V.; Pettitt, M. NMR and quenched molecular dynamics studies of superpotent linear and cyclic α-melanotropins. *J. Peptide Res.* **1998**, *51*, 420−431.

(74) O'Connor, S.; Smith, P.; Al-Obeidi, F.; Pettitt, B. M. Quenched Molecular Dynamics Simulations of Tuftsin and Proposed Cyclic Analogues. *J. Med. Chem.* **1992**, *35*, 2870−2881.

(75) Maraval, V.; Laurent, R.; Donnadieu, B.; Mauzac, M.; Caminade, A. M.; Majoral, J. P. Rapid synthesis of phosphorus-containing dendrimers with controlled molecular architectures: First example of surface-block, layer-block, and segment-block dendrimers issued from the same dendron. *J. Am. Chem. Soc.* **2000**, *122*, 2499−2511.

(76) Moore, J. S. Shape-Persistent Molecular Architectures of Nanoscale Dimension. *Acc. Chem. Res.* **1997**, *30*, 402−413.

(77) Pesak, D. J.; Moore, J. S. Columnar Liquid Crystals from Shape-Persistent Dendritic Molecules. *Angew. Chem., Int. Ed. Engl.* **1997**, *36*, 1636−1639.

AR000044C